Vol 459|25 June 2009|doi:10.1038/nature08115

LETTERS

High-speed tracking of rupture and clustering in freely falling granular streams

John R. Royer[1], Daniel J. Evans[1], Loreto Oyarte[1], Qiti Guo[1], Eliot Kapit[1], Matthias E. Möbius[1]†, Scott R. Waitukaitis[1] & Heinrich M. Jaeger[1]

Thin streams of liquid commonly break up into characteristic droplet patterns owing to the surface-tension-driven Plateau–Rayleigh instability[1–3]. Very similar patterns are observed when initially uniform streams of dry granular material break up into clusters of grains[4–6], even though flows of macroscopic particles are considered to lack surface tension[7,8]. Recent studies on freely falling granular streams tracked fluctuations in the stream profile[9], but the clustering mechanism remained unresolved because the full evolution of the instability could not be observed. Here we demonstrate that the cluster formation is driven by minute, nanoNewton cohesive forces that arise from a combination of van der Waals interactions and capillary bridges between nanometre-scale surface asperities. Our experiments involve high-speed video imaging of the granular stream in the co-moving frame, control over the properties of the grain surfaces and the use of atomic force microscopy to measure grain–grain interactions. The cohesive forces that we measure correspond to an equivalent surface tension five orders of magnitude below that of ordinary liquids. We find that the shapes of these weakly cohesive, non-thermal clusters of macroscopic particles closely resemble droplets resulting from thermally induced rupture of liquid nanojets[10–12].

Granular systems in Hele–Shaw geometries or impinging on stationary targets have recently been shown to provide excellent approximations of liquid behaviour in the limit approaching zero surface tension[7,8]. In these experiments, however, the material was strongly forced and momentum transfer dominated other forces. To observe the vestiges of any residual surface tension and estimate its magnitude requires conditions where the material experiences as little external forcing as possible. Motivated by the strikingly liquid-like appearance of streams of fine-grained granular material breaking into droplets, first reported in 1890 (ref. 13) and more recently observed within the context of granular jets[4,5], we investigated freely falling granular streams, analogous to liquids falling from a faucet. These streams provide a controlled system for the study of droplet formation provided that break-up events can be tracked with high spatial resolution at high imaging speeds. The difficulty is that the time to break-up increases rapidly with decreasing surface tension. For granular streams this requires tracking grains for half a metre or more before they form clusters. We achieve this using a high-speed video camera that falls with the stream and report here on experiments capturing the granular break-up dynamics in detail.

Figure 1 shows the break-up process for a stream of glass spheres emerging from a small opening in the bottom of a hopper mounted inside a 2.5-m-tall, evacuated cylinder (Fig. 1a). As the stream accelerates under gravity, an axial velocity gradient develops and elongates the stream as it falls. While the stream stretches, initial

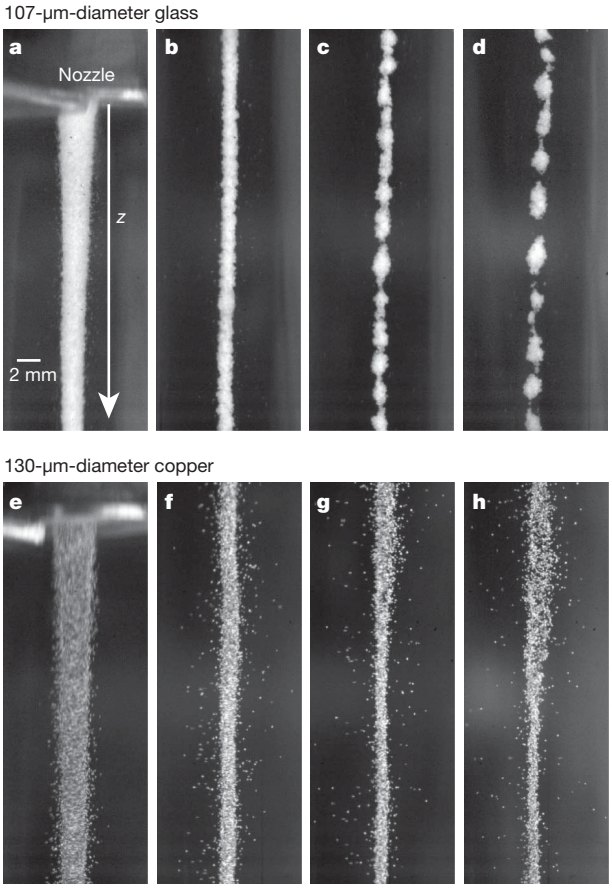

Figure 1 | Break-up of a granular stream. a–d, Stream of glass grains of diameter $d = 107\ \mu m \pm 19\ \mu m$ falling out of a nozzle of diameter $D_0 = 4.0$ mm at the following points: just below the nozzle (**a**), and $z = 20$ cm (**b**), $z = 55$ cm (**c**) and $z = 97$ cm (**d**) from the top of the frame to the nozzle. **e–h**, Stream of copper grains of diameter $d = 130\ \mu m \pm 30\ \mu m$ falling out of the same $D_0 = 4$ mm nozzle at the following points: just below the nozzle (**e**), and $z = 20$ cm (**f**), $z = 55$ cm (**g**) and $z = 97$ cm (**h**) from the top of the frame to the nozzle. The nozzle and reservoir of grains are housed in a 2.5-m-tall acrylic tube, which is sealed and evacuated to 0.03 kPa (gas mean free path, $\sim 200\ \mu m$) to reduce air drag. We use a high-speed camera (Phantom v7.1) falling along a low-friction rail outside of the chamber to track a 3-cm-long section of the stream as it falls from the nozzle to the bottom of the chamber (0.04 mm per pixel, 1,000 frames per second; see Supplementary Movies). An optical encoder measures the position of the camera, allowing us to correct for small deviations from free-fall as the camera moves along the rail.

[1]James Franck Institute and Department of Physics, The University of Chicago, Chicago, Illinois 60637, USA. †Present address: School of Physics, Trinity College Dublin, Dublin 2, Ireland.

undulations emerge and deepen (Fig. 1b), creating clusters connected by thin bridges a few grains wide (Fig. 1c). These bridges eventually rupture as the clusters continue to separate (Fig. 1d). This ability to track the evolution of individual clusters over several metres and image the rupture details provides unique insights into the underlying clustering mechanism.

Whereas the instability of ordinary liquid columns is driven by molecular surface tension, possible mechanisms for droplet formation in granular systems include hydrodynamic interactions with the surrounding gas, inelastic grain–grain collisions, and cohesive forces. Hydrodynamic interactions have indeed recently been associated with fluctuations in the profile of streams falling in air[9]; however, from experiments across a wide range of ambient pressures down to 0.03 kPa we find that grain–gas interactions do not drive clustering (Supplementary Fig. S1), in agreement with earlier work[6]. Inelastic collisions are known to produce clusters in other granular systems[14–16], although for realistic grains, where the coefficient of restitution approaches unity at low velocities, these clusters may be transient. To vary the inelasticity, we replaced the glass spheres by copper grains of similar size. The grain mass does not enter scenarios solely driven by inelasticity, so the smaller coefficient of restitution (for copper[17], $e \approx 0.90$, for soda lime glass[18], $e \approx 0.97$ at impact velocities of 0.5–1.0 m s^{-1}) should lead to even more pronounced clustering. As shown in Fig. 1e–h, the opposite behaviour is observed: Instead of breaking up into discrete, compact clusters, sections of the stream begin to drift apart and expand in the radial direction.

In principle, cohesion might arise from a variety of sources, including electrostatic charging, capillary or van der Waals forces[19–21]. For a rough estimate of the cohesive strength we track clusters as they fall and accelerate to a speed at which Stokes drag pulls individual grains off cluster protrusions. Correcting for slight changes in the air viscosity at reduced pressure, this gives values of a few nanoNewtons. To compare this to any electrostatic forces present, we obtain the distribution of charges on the grains by applying a uniform electric field perpendicular to the falling stream and tracking individual grain trajectories (see Supplementary Information). For both glass and copper, we find the streams are neutral overall but contain a small fraction of positively and negatively charged grains, up to a roughly $q_{max} = \pm 100{,}000$ electron charges per grain (Supplementary Fig. S2). Still, this gives attractive electrostatic forces a maximum $F_{max} = (1/4\pi\varepsilon_0)q_{max}^2/d^2 \approx 0.1$ nN for grains with diameter $d = 100$ μm, too weak to be the dominant cohesive force. (Here $\varepsilon_0 = 8.85 \times 10^{-12}$ C^2 N^{-1} m^{-2} is the permittivity of free space.) Furthermore, experiments with conductive, silver-coated 100-μm-diameter glass spheres produce clusters identical to experiments using uncoated spheres, emphasizing that electrostatic forces do not drive the observed clustering.

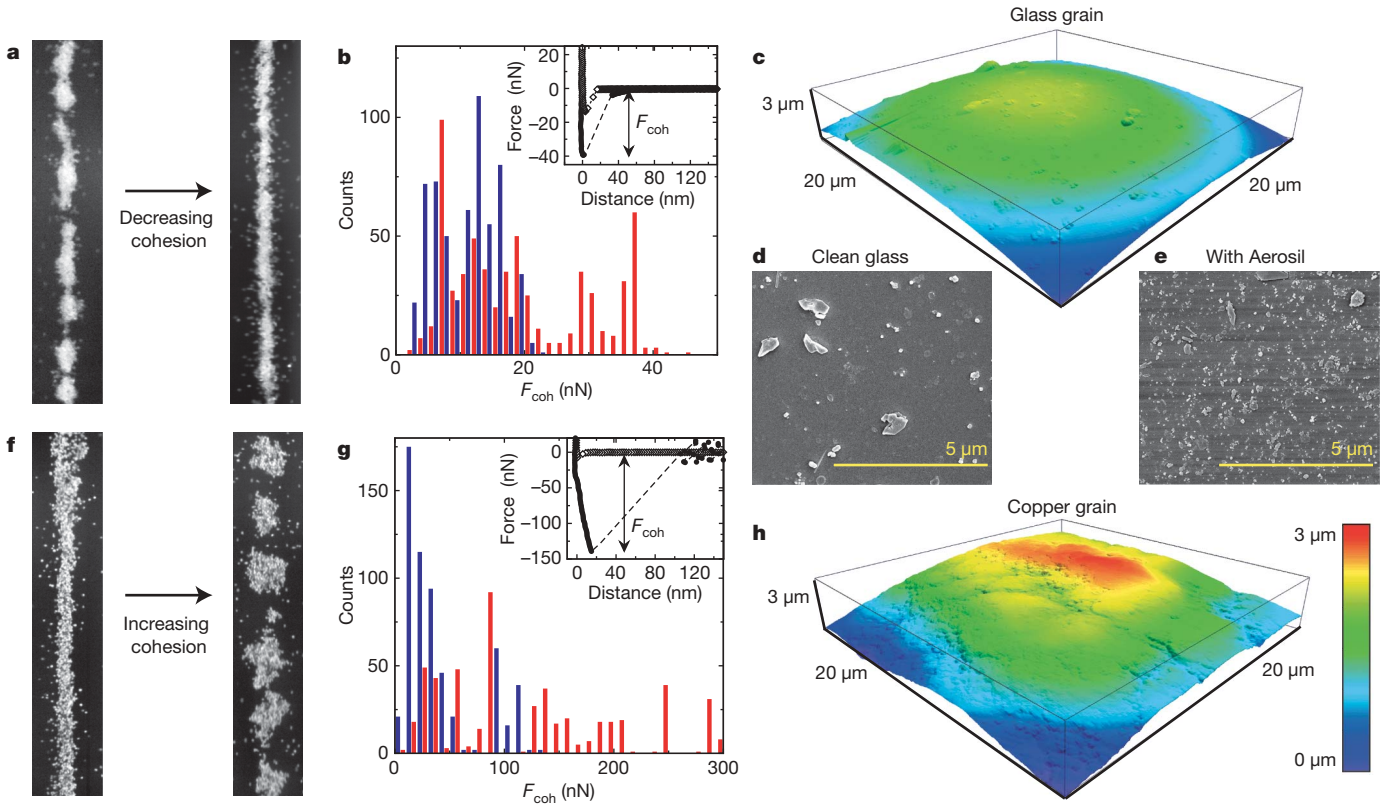

Figure 2 | Controlling clustering by altering cohesion. **a**, Stream of glass grains of diameter $d = 151$ μm $\pm$ 26 μm (left) and the same grains coated with silica particles of size 10–100 nm (Aerosil 200, Degussa) (right). Aerosil is a common additive used to improve the flowability of powders by reducing cohesion. The addition of Aerosil altered but did not eliminate clustering in finer glass grains of diameter 107 μm or 54 μm. **b**, Histograms of cohesive forces between pairs of grains for untreated, clean glass grains (blue) and Aerosil-coated grains (red). Forces were measured using an Asylum Research MFP-3D-Bio AFM. Single grains were epoxy-glued to the AFM cantilever (Nanosensors, spring constant $k \approx 2$ N m^{-1}) and brought into contact with fixed grains of the same material. The inset to **b** shows a typical force–displacement curve for a pair of untreated glass grains, showing the approach (open symbols) and retraction (closed symbols) of the cantilever. F_{coh} is the maximum force magnitude before two grains abruptly snap apart during retraction (dotted lines). Each histogram consists of measurements from 20 separate force curves from 15 different grains. **c**, AFM topographic map of 20 μm × 20 μm section of an untreated glass grain. **d**, **e**, Scanning electron microscope images of an untreated glass grain (**d**) and a grain coated with Aerosil (**e**). The grains were coated by mixing a small amount (~0.1% by weight) of Aerosil with untreated grains. Scanning electron microscope imaging of random samples confirmed that the Aerosil was well dispersed across the grain surfaces. **f**, Stream of copper grains of diameter $d = 130$ μm $\pm$ 30 μm (left) and the same copper mixed with a small amount of oil (right). **g**, Histogram of pull-off forces for untreated grains (blue) and oil coated grains (red). The inset to **g** shows a force–displacement curve illustrating the larger pull-off force from oil-coated grains and the measurable displacement of the grain before it snaps off the surface. **h**, AFM topographic map of a 20 μm × 20 μm section of a copper grain.

To determine the intergrain cohesive forces F_{coh} directly, we record force–displacement curves of individual grains brought into contact and pulled apart by an atomic force microscope (AFM)[22,23] (Fig. 2). F_{coh} varies across different grains, but is generally a few tens of nanoNewtons, in agreement with our earlier estimate. Both van der Waals and capillary forces for perfectly smooth spheres in contact scale as $F_{coh} \propto \gamma d$, with interfacial energy γ of the order of tens of milliNewtons per metre (ref. 19), giving microNewton forces for grains of diameter $d = 150\,\mu m$. The orders-of-magnitude-smaller forces observed (Fig. 2b, g), as well as the absence of any scaling of F_{coh} with grain diameter, emphasize the significance of the local, nanometre-scale grain topography[23,24]. It is difficult to distinguish van der Waals from capillary forces because we cannot rule out molecularly thin absorbed films that create tiny bridges between individual asperities[24,25]. However, we still observe clustering in glass grains stored under vacuum (0.05 kPa) at low humidity (<1%) and also in grains coated with hydrophobic silane.

To confirm that tiny, short-ranged cohesive forces are responsible for the clustering, we can decrease their strength by enhancing the grains' surface roughness. As shown in Fig. 2 for 150-μm-diameter glass grains, adding nanoscale asperities to the grain surfaces reduces F_{coh} by roughly a factor of two and indeed reduces clustering significantly. However, what controls clustering cannot be determined solely from knowledge of F_{coh}. In fact, although clean glass does form clusters, F_{coh} for glass is not larger than for copper grains with similar mass (median values are 17 nN and 30 nN, respectively; see Fig. 2). One reason is that AFM pull-off force measurements only mimic head-on collisions, while both normal and tangential force components must be considered to describe fully the collision of macroscopic bodies. Topographic maps show significant differences in the nature of the roughness (Fig. 2c, h), and the much more pronounced large-scale roughness for copper is likely to reduce sliding, leading to different rotational collision dynamics. For coarse sand, rough and irregular like copper, we indeed observe weaker, less compact clusters (Supplementary Information).

We can greatly simplify the picture and eliminate many of the complications associated with dissipation due to sliding or rolling when 'sticky' collisions are the dominant source of energy loss. In this scenario, inelastic interactions initially reduce the relative particle velocities δu to a level where colliding grains with mass m get captured

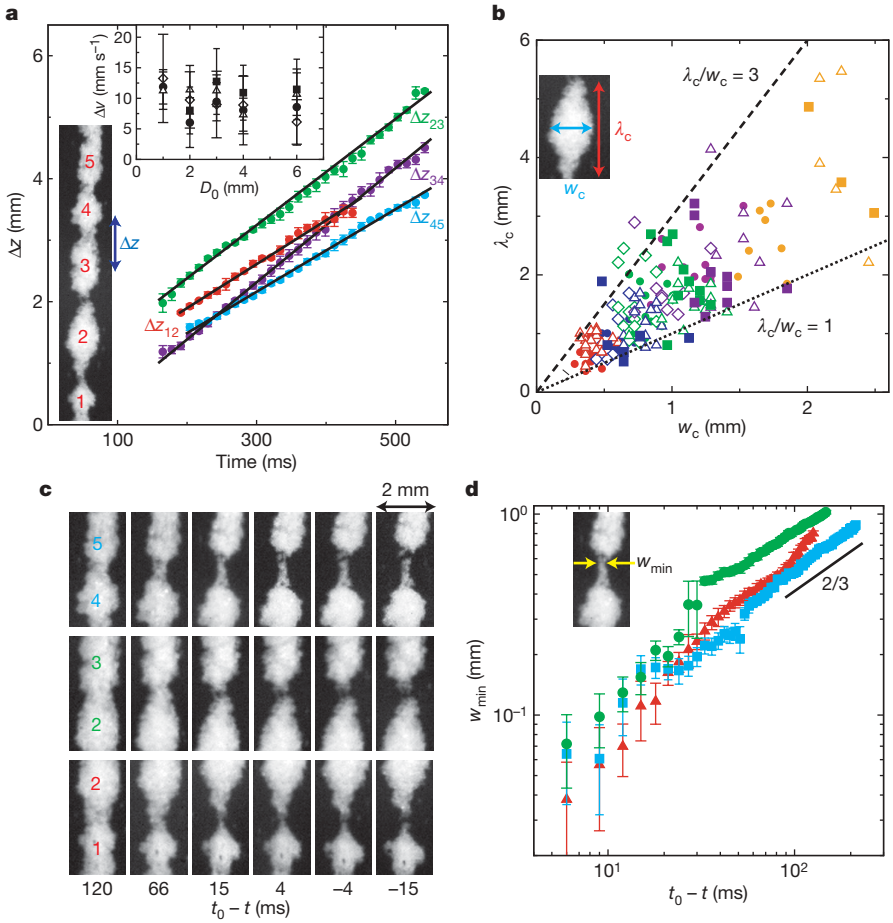

Figure 3 | Clustering dynamics. **a**, Separation of clusters Δz versus time t (see diagram) for representative sample of five adjacent clusters from the stream shown in Fig. 1a–d (107-μm-diameter glass, $D_0 = 4$ mm). Δz was measured by tracking local maxima in the width of the stream both before and after the clusters separated. $t = 0$ corresponds to the time where each section of the stream left the nozzle. Solid lines show fits to $\Delta z(t) = \Delta z_0 + (\Delta v)t$. Linear growth was observed for all nozzle diameters and grain materials. The inset to **a** shows the median separation velocity Δv obtained from fits to $\Delta z(t)$ versus nozzle diameter D_0 for glass spheres of $d = 54\,\mu m \pm 10\,\mu m$ (open triangles), $d = 107\,\mu m \pm 19\,\mu m$ (solid circles), $d = 151\,\mu m \pm 26\,\mu m$ (open diamonds), and oil-coated copper particles of $d = 130\,\mu m \pm 30\,\mu m$ (solid squares). **b**, Cluster length λ_c versus cluster width w_c (see diagram) for individual clusters. Different grain materials are represented by the same symbols as in **a**. Different nozzle diameters are colour-coded: $D_0 = 1.0$ mm (red), 2.0 mm (blue), 2.9 mm (green), 4.0 mm (purple) and 6.1 mm (orange). **c**, Thinning and rupture of the neck between adjacent clusters for three of the pairs of clusters from **a**. Rupture time t_0 is the first frame where an open gap appears between clusters. From the time each section of the stream left the nozzle, $t_0 = 421$ ms (pair 4–5), 325 ms (pair 2–3) and 350 ms (pair 1–2). **d**, Log–log plot of the minimum neck diameter w_{min} (see diagram) versus time to rupture for each of the pairs of clusters in **c**: pair 4–5 (blue), pair 2–3 (green) and pair 1–2 (red). Solid line with a slope of +2/3 drawn for comparison. Error bars on Δz and w_{min} indicate statistical errors from averaging over multiple frames. Error bars on Δv show the standard deviation based on 6–10 pairs of clusters from a single experiment.

by cohesive trapping potentials. This happens when the pre-collision kinetic energy or 'granular temperature' $(m/2)(\delta u)^2$ becomes smaller than $W_{coh} = \int F_{coh}(\xi)d\xi$, the work done against a cohesive force $F_{coh}(\xi)$ as two particles try to separate themselves by a distance ξ (refs 26, 27). This energy loss to cohesion prevents the coefficient of restitution from approaching unity at low velocities, instead causing it to rapidly drop to zero as the collision velocity approaches $v_c = (2W_{coh}/m)^{1/2}$.

This scenario can be tested quantitatively by using rough grains (to reduce sliding) and adding cohesion (to induce sticking). To do this, we mixed copper grains with a small amount ($\sim 3 \times 10^{-4}$ by volume) of mineral oil, amounting to a 10-nm-thick coat on average. As Fig. 2 shows, this results in a fivefold increase of the median pull-off force for copper, which now clusters very similarly to glass. Tracing $F_{coh}(\xi)$ over 10–20 nm we calculate $W_{coh} \approx 10^{-15}$ J. The velocity threshold for sticking collisions between two copper grains (density $\rho = 8.9\,kg\,m^{-3}$, $d = 130\,\mu m$) is then $v_c = (2W_{coh}/m)^{1/2} \approx 0.4\,mm\,s^{-1}$. This value agrees well with upper limits on the relative particle velocities inside clusters obtained from direct imaging. For example, for the glass data in Fig. 1, from the appearance of undulations (Fig. 1b) to the fully formed clusters (Fig. 1d) 240 ms later, the maxima in the stream width change by <0.1 mm, limiting δu to less than $0.5\,mm\,s^{-1}$ inside clusters. It also explains the absence of clustering when the velocity fluctuations are much larger, for example, at the nozzle where $\delta u \approx 1\,cm\,s^{-1}$ for both glass and copper as determined directly by particle imaging velocimetry.

We can use our results to estimate an equivalent 'granular' surface tension γ. In a conventional liquid, surface tension scales as $\gamma \approx \varepsilon/\sigma^2$, where ε is the depth of the attractive potential between molecules and σ is their size[28]. Using W_{coh} instead of ε and d instead of σ, we find $\gamma \approx 0.1\,\mu N\,m^{-1}$, which is five orders of magnitude lower than in conventional liquids. To the extent that the granular streams behave like liquids, our experiments can therefore probe an ultralow-surface-tension regime that has recently attracted attention—such as simulations of nanojets[10–12], and colloidal systems a few molecules or particles wide[29]. For liquids in this regime, thermal fluctuations are sufficient to drive break-up. Intriguingly, the granular cluster shapes exhibit striking similarities, including characteristic double-cone necks at break-up.

To explore these connections quantitatively, we track details of the break-up between pairs of clusters (Fig. 3). The separation velocity between any two clusters varies significantly, as does the cluster size and the precise shape of the necks; on average, however, separation speed, cluster aspect ratio and neck evolution exhibit remarkably robust behaviour, largely independent of grain type, grain size or nozzle diameter. Independently of surface tension, in both macroscopic and nanoscale liquid streams, perturbations are unstable only for wavelengths λ greater than the stream circumference πw (refs 2, 10, 12). For all granular streams studied, the ratio of cluster length λ_c to cluster width w_c instead appears to be smaller, falling between one and three (Fig. 3b). This narrow interval is independent of experimental details, which might explain why similar clusters also form under quite different initial conditions, for example, in granular jets formed by sphere impact[4,5]. Finally, Fig. 3c and d shows the evolution of three different necks taken from a small section of the granular stream. In liquid nano-threads the minimum neck width is predicted[30] to scale as $w_{min} \propto (t_0 - t)^{0.418}$ with time to break-off at t_0. While our data range is too small to claim any particular scaling, the data nevertheless appear incompatible with exponents $<1/2$. At early times the data seem much more in line with inviscid break-up (exponent 2/3) of macroscopic liquid streams[2], although there the neck shapes are quite different[1].

These experimental results open up new territory for which there is at present no theoretical framework. The granular streams act like dense, cold fluids. The low temperature allows us to observe the exceedingly weak cohesive forces responsible for clustering and extract an effective, ultralow surface tension. Although the break-up shapes are similar to those seen in simulations of mesoscopic liquid threads such as nanojets, the clustering results from collisional cooling rather than thermal fluctuations. Given that freely falling granular streams are exquisitely sensitive probes for minute forces they also provide a new tool with which to measure cohesive energies in granular systems.

Received 22 February; accepted 5 May 2009.

1. Shi, X. D., Brenner, M. P. & Nagel, S. R. A cascade of structure in a drop falling from a faucet. *Science* **265,** 219–222 (1994).
2. Eggers, J. & Villermaux, E. Physics of liquid jets. *Rep. Prog. Phys.* **71,** 036601 (2008).
3. Doshi, P. *et al.* Persistence of memory in drop breakup: the breakdown of universality. *Science* **302,** 1185–1188 (2003).
4. Lohse, D. *et al.* Impact on soft sand: void collapse and jet formation. *Phys. Rev. Lett.* **93,** 198003 (2004).
5. Royer, J. R. *et al.* Formation of granular jets observed by high-speed X-ray radiography. *Nature Phys.* **1,** 164–167 (2005).
6. Möbius, M. E. Clustering instability in a freely falling granular jet. *Phys. Rev. E* **74,** 051304 (2006).
7. Cheng, X., Xu, L., Patterson, A., Jaeger, H. M. & Nagel, S. R. Towards the zero-surface-tension limit in granular fingering instability. *Nature Phys.* **4,** 234–237 (2008).
8. Cheng, X., Varas, G., Citron, D., Jaeger, H. M. & Nagel, S. R. Collective behavior in a granular jet: emergence of a liquid with zero surface tension. *Phys. Rev. Lett.* **99,** 188001 (2007).
9. Amarouchene, Y., Boudet, J.-F. & Kellay, H. Capillarylike fluctuations at the interface of falling granular jets. *Phys. Rev. Lett.* **100,** 218001 (2008).
10. Koplik, J. & Banavar, J. R. Molecular dynamics of interface rupture. *Phys. Fluids A* **5,** 521–536 (1993).
11. Moseler, M. & Landman, U. Formation, stability, and breakup of nanojets. *Science* **289,** 1165–1169 (2000).
12. Kawano, S. Molecular dynamics of rupture phenomena in a liquid thread. *Phys. Rev. E* **58,** 4468–4472 (1998).
13. Khamontoff, N. Application of photography to the study of the structure of trickles of fluid and dry materials. *J. Russ. Phys-Chem. Soc.* **22,** 281–284 (1890).
14. Goldhirsch, I. Rapid granular flows. *Annu. Rev. Fluid Mech.* **35,** 267–293 (2003).
15. Brilliantov, N. V. & Pöschel, T. *Kinetic Theory of Granular Gases* (Oxford University Press, 2004).
16. Efrati, E., Livne, E. & Meerson, B. Hydrodynamic singularities and clustering in a freely cooling inelastic gas. *Phys. Rev. Lett.* **94,** 088001 (2005).
17. Kuwabara, G. & Kono, K. Restitution coefficient in a collision between two spheres. *Jpn. J. Appl. Phys.* **26,** 1230–1233 (1987).
18. Foerster, S. F., Louge, M. Y., Chang, H. & Allia, K. Measurements of the collision properties of small spheres. *Phys. Fluids* **6,** 1108–1115 (1994).
19. Israelachvili, J. N. *Intermolecular and Surface Forces* 2nd edn (Academic Press, 1992).
20. Podczeck, F. *Particle-Particle Adhesion in Pharmaceutical Powder Handling* (Imperial College Press, 1998).
21. Visser, J. Van der Waals and other cohesive forces affecting powder fluidization. *Powder Technol.* **58,** 1–10 (1989).
22. Jones, R. From single particle AFM studies of adhesion and friction to bulk flow: forging the links. *Granular Matter* **4,** 191–204 (2003).
23. Schaefer, D. M. *et al.* in *Fundamentals of Adhesion and Interfaces* (eds Rimai, D. S., Demejo, L. P. & Mittal, K. L.) 35–48 (VSP, 1995).
24. Halsey, T. C. & Levine, A. J. How sandcastles fall. *Phys. Rev. Lett.* **80,** 3141–3144 (1998).
25. Bocquet, L., Charlaix, E., Ciliberto, S. & Crassous, J. Moisture-induced ageing in granular media and the kinetics of capillary condensation. *Nature* **396,** 735–737 (1998).
26. Brilliantov, N. V., Albers, N., Spahn, F. & Pöschel, T. Collision dynamics of granular particles with adhesion. *Phys. Rev. E* **76,** 051302 (2007).
27. Sorace, C. M., Louge, M. Y., Crozier, M. D. & Law, V. H. C. High apparent adhesion energy in the breakdown of normal restitution for binary impacts of small spheres at low speed. *Mech. Res. Commun.* **36,** 364–368 (2009).
28. Rowlinson, J. S. & Widom, B. *Molecular Theory of Capillarity* (Clarendon Press, 1982).
29. Hennequin, Y. *et al.* Drop formation by thermal fluctuations at an ultralow surface tension. *Phys. Rev. Lett.* **97,** 244502 (2006).
30. Eggers, J. Dynamics of liquid nanojets. *Phys. Rev. Lett.* **89,** 084502 (2002).

Supplementary Information is linked to the online version of the paper at www.nature.com/nature.

Acknowledgements We thank X. Cheng, R. Cocco, E. Corwin, R. Karri, N. Keim, T. Knowlton, S. Nagel, T. Witten and W. Zhang for discussions and J. Jureller for AFM training and assistance. This work was supported by NSF through its MRSEC programme and the Inter-American Materials Collaboration Chicago-Chile, and by the Keck Initiative for Ultrafast Imaging at the University of Chicago.

Author Information Reprints and permissions information is available at www.nature.com/reprints. Correspondence and requests for materials should be addressed to J.R.R. (jroyer@uchicago.edu).